

High-order harmonic generation from diatomic molecules with large internuclear distance: The effect of two-center interference

Y. J. Chen¹, J. Liu^{1*}

1. Institute of Applied Physics and Computational Mathematics, P.O.Box 100088, Beijing, P. R. China

2. Graduate School, China Academy of Engineering Physics,

P.O. Box 8009-30, Beijing, 100088, P. R. China

(Dated: October 28, 2018)

In the present paper, we investigate the high-order harmonic generation (HHG) from diatomic molecules with large internuclear distance using a strong field approximation (SFA) model. We find that the hump and dip structure emerges in the plateau region of the harmonic spectrum, and the location of this striking structure is sensitive to the laser intensity. Our model analysis reveals that two-center interference as well as the interference between different recombination electron trajectories are responsible for the unusual enhanced or suppressed harmonic yield at a certain order, and these interference effects are greatly influenced by the laser parameters such as intensity.

PACS numbers: 42.65.Ky, 32.80.Rm

I. INTRODUCTION

The high-order harmonic generation (HHG) from atoms and molecules has been one of the most intensely studied aspects of strong-field physics[1, 2, 3, 4, 5, 6, 7, 8, 9, 10, 11, 12, 13, 14, 15], because it can be applied as a coherent ultrashort radiation source in the extreme ultraviolet(XUV) and soft x-ray regions[16]. Due to the multi-center characteristics and greater freedom, the molecules show more complicated structures in their HHG spectrum than atoms and the dynamics of molecules in the external field is more difficult to investigate.

Among many treatments, the semiclassical recollision model[17] is an applaudable theory that provides a appropriate picture for HHG. In this model, the high harmonics are generated by a three-step sequence: (1) tunnel ionization of the highest energy of the electron, (2) acceleration of the free electron in the laser field, and driving the electron back to the parent ion, (3) recombination of the electron to the state from which it originated. The recombination step leads to the emission of a XUV photon whose energy is given by the sum of the electron of kinetic energy plus the ionization potential of the state. A widely used semianalytical approach to describe HHG is the strong field approximation (SFA) or Lewenstein model [18], which is applicable to the molecules. It can be regarded as the quantum mechanical version of the semi-classical recollision model. The Lewenstein model has the advantage of requiring less computational effort than the *ab initio* solution of the time-dependent Schrödinger equation, which becomes very demanding at high laser intensities. Another advantage of the model is that it yields a physical interpretation of the underlying mechanisms and a certain degree of analytical description.

Recently, several theoretical and experimental reports study two-center interference on the HHG from molecules of H_2^+ [1, 2, 3, 4] and CO_2 [5, 6, 7, 8]. Lein *et al* observed the phenomenon and attributed it to the returning electron wave colliding with cores of the two-center molecule, where an interference occurs[1]. They found that the

interference effects are sensitive to the molecular orientation but not to the laser parameters. Ciappina *et al* use the SFA model to study two-center interference[13]. They compared the SFA prediction of the interference-minimum position to the exact value obtained from the *ab initio* calculations. They observe that using the two-center continuum wave functions, instead of a plane wave to describe the continuum electron, greatly improves the comparison. The usage of the continuum wave functions can be considered an attempt to account for Coulomb effects on the returning electron.

The previous discussions, however, are mainly toward the molecules with small internuclear distance R . Detailed investigations for the interference effects on HHG from molecules with large R are still in lack. For the large internuclear distance case, strong coupling between the ground state and the first excited state emerges due to charge-resonance effect[12]. This could complicate the HHG process.

In the present paper, using a SFA model that considers the Coulomb effects, we investigate the HHG from a 1D model diatomic molecule with large R (16 a.u.). The SFA model calculation gives the HHG spectrum qualitatively consistent with the numerical result and shows the pronounced hump and dip structure in the plateau region. Detailed analysis shows that two-center interference as well as the interference between different recombination electron trajectories are responsible for the enhanced or suppressed harmonic yield at a certain order. And in particular, the location of the unusual structure is found to be sensitive to the laser intensity.

This paper is organized as follows. In Sec.II, we present our analytical theory. In Sec.III, we apply our theory to the HHG from a 1D model diatomic molecule with large R . We also analyze the complicated interference patterns here. Sec.IV is our conclusion.

II. ANALYTIC THEORY

In Ref.[12], we have developed a SFA model for the HHG from symmetric diatomic molecules, emphasizing the influence of the charge-resonance states that are strongly coupled to electromagnetic fields for the case of large R . And we showed there that for sufficiently large internuclear distances, while initially the system is in the ground state, the contribution to the harmonic comes mostly from the continuum state-ground state transition. For very large R with $\mathbf{D} \approx 0$, where $\mathbf{D} = \langle 0|\hat{\mathbf{p}}|1\rangle$, $|0\rangle$ and $|1\rangle$ are the ground state and the first excited state of the unperturbed system, respectively, the harmonic formula along the field direction can be written as

$$P(\omega') = i \int d\mathbf{p} |\mathbf{A}_0| \pi \langle 0|\mathbf{p}\rangle (\mathbf{p} \cdot \hat{\mathbf{e}})^2 \langle \mathbf{p}|0\rangle \sum_{n,m=-\infty}^{n,m=+\infty} \left\{ \frac{\delta[(m-1+n)\omega - \omega']}{A} + \frac{\delta[(m+1+n)\omega - \omega']}{B} \right\} J_n J_m, \quad (1)$$

where $J_n = J_n(\frac{-\mathbf{p} \cdot \mathbf{A}_0}{\omega})$, $J_m = J_m(\frac{\mathbf{p} \cdot \mathbf{A}_0}{\omega})$, $A = (m-1)\omega - \frac{\mathbf{p}^2}{2} - E_0$, $B = (m+1)\omega - \frac{\mathbf{p}^2}{2} - E_0$. E_0 is the ionization potential of the ground state, $\mathbf{A}_0 = E\hat{\mathbf{e}}/\omega$. E is the field amplitude, $\hat{\mathbf{e}}$ is the unit vector along the field direction, ω is the field frequency. Eq. (1) is applicable for the large internuclear distance and the weak field as discussed in our previous paper. In the SFA[18], an important assumption is that electrons in the continuum states can be treated as a free particle moving in the electric field without considering the Coulomb potential. Accordingly, the continuum wave function $|\mathbf{p}\rangle$ is approximated by a plane wave $|\mathbf{p}\rangle = e^{i\mathbf{p} \cdot \mathbf{r}}$ with the energy $E_{\mathbf{p}} = \mathbf{p}^2/2$, where the binding potential is completely omitted. Here, we extend to consider the modification from the Coulomb potential, thus a better approximation of the continuum states in the following form is exploited,

$$|\mathbf{p}\rangle = e^{i\mathbf{p}_{\mathbf{k}} \cdot \mathbf{r}}, \quad (2)$$

where the effective momentum $\mathbf{p}_{\mathbf{k}} = \mathbf{p} \sqrt{\mathbf{p}^2 + 2E_0}/|\mathbf{p}|$, and the energy $E_{\mathbf{p}} = \mathbf{p}^2/2$. This incorporates some effects of the binding potential through its dependence on E_0 [2, 4, 15, 19]. With the rectification of Eq. (2), the harmonic formula of Eq. (1) can be rewritten as

$$P(\omega') = i \int d\mathbf{p} |\mathbf{A}_0| \pi \langle 0|\mathbf{p}_{\mathbf{k}}\rangle (\mathbf{p} \cdot \hat{\mathbf{e}})^2 \langle \mathbf{p}_{\mathbf{k}}|0\rangle \sum_{n,m=-\infty}^{n,m=+\infty} \left\{ \frac{\delta[(m-1+n)\omega - \omega']}{A} + \frac{\delta[(m+1+n)\omega - \omega']}{B} \right\} J_n J_m, \quad (3)$$

For comparison with 1D numerical simulation, the model is simplified to an one dimensional model and the integral over the momentum is evaluated by the so-called pole approximation[20] throughout this paper. By setting $A = 0$ or $B = 0$, which denotes the energy conservation in the ionization process, one can obtain the

momentum \mathbf{p} with certain m . The two *delta* functions in Eq. (3) denote the emission of harmonics with certain m and n in the recombination process. From the above explicit expression, we conclude that the recombination electrons with diverse momenta could contribute to a common harmonic order, since the *delta* functions explicitly depend on the integer n . This implies that, not only in the ionization process the electron can absorb $m \pm 1$ photons, but also in the recombination process the electron can absorb (positive) or emit (negative) n photons, which induces the final emission of $m \pm 1 + n$ photons.

The integrand of Eq. (3) can be divided into several parts. The part of $\langle 0|\mathbf{p}_{\mathbf{k}}\rangle (\mathbf{p} \cdot \hat{\mathbf{e}})^2 \langle \mathbf{p}_{\mathbf{k}}|0\rangle$ explicitly depends on the ionization energy E_0 and the internuclear distance R , but is independent of the field parameters. It incorporates the interference effects between cores of the two-center molecules [2, 21], and mainly is determined by the properties of the molecules. The part of $J_n J_m$ explicitly depends on the field amplitude E and the field frequency ω , representing the probability amplitude for an electron to absorb or emit $n + m \pm 1$ photons. It reflects the interaction between the electron and the field and is closely related to the field parameters. Thus, those recombination electrons that have the momenta satisfying the condition of $A = 0$ or $B = 0$ all could contribute to a harmonic order, and the weight of the contribution depends on not only two-center interference but also the interference between different recombination electron trajectories[18]. The latter is strongly depends on the laser intensity, as a result, we expect that the interference structure in HHG spectra could rely on the field parameters. The above theoretical analysis is verified by our numerical simulations as shown in following.

III. NUMERICAL RESULTS

The Hamiltonian of the 1D model diatomic molecule studied here is $H(t) = -\frac{d^2}{2dx^2} - \frac{Z}{\sqrt{1.44+(x+0.5R)^2}} - \frac{Z}{\sqrt{1.44+(x-0.5R)^2}} - x\mathcal{E} \sin(\omega t)$, where Z is the effective charge, R is the internuclear separation, \mathcal{E} is the amplitude of the external electric field, and ω is the frequency of the external field. In the paper, we adopt the atomic units, $\hbar = e = m_e = 1$. Calculations have been performed for 780 nm trapezoidally shaped laser pulses with a total duration of 10 optical cycles and linear ramps of three optical cycles. Numerically, the above Schrödinger equation can be solved by the operator-splitting method[22].

A typical result is presented in Fig. 1. Here we plot the harmonic spectra of a 1D model diatomic molecule with $Z = 1$, $R = 16$ a.u. and $E_0 = 0.638$ a.u. at the field intensity $I = 5.3 \times 10^{13} \text{W/cm}^2$ (Figs. 1(a) and (c)) and $I = 1 \times 10^{14} \text{W/cm}^2$ (Figs. 1(b) and (d)). Figs. 1(a) and (b) are the numerical results and Figs. 1(c) and (d) are the analytic results calculated by Eq. (3). The min-

imum or dip structure is at the 17th and the 15th order in Figs. 1(a) and (c), respectively, and that in Figs. 1(b) and (d) both are at the 23rd order, as indicated by the vertical arrows. Though there are some differences in the accurate positions of the minimum between the analytic and the numerical results, the dip structure can be distinguished in all plottings of the spectra. In addition, a hump structure around the 11th order harmonic in Figs. 1(a), around the 15th order harmonic in Figs. 1(b), around the 9th order harmonic in Figs. 1(c), and around the 13th order harmonic in Figs. 1(d), can be identified, as indicated by the horizontal arrows.

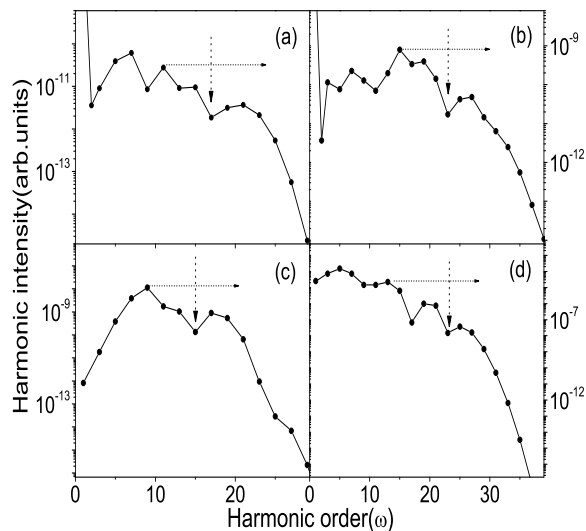


Figure 1: Photon-emission spectra of a symmetrical diatomic molecule with $Z = 1$, $R = 16$ a.u. and $E_0 = 0.638$ a.u. at the field intensity $I = 5.3 \times 10^{13} \text{W/cm}^2$ (Figs. 1(a) and (c)) and $I = 1 \times 10^{14} \text{W/cm}^2$ (Figs. 1(b) and (d)). (a) and (b): The numerical results; (c) and (d): the analytic results calculated by Eq. (3). See the context for the illumination of the arrows.

In Fig. 2, we plot the harmonic spectra of a 1D model diatomic molecule with $Z = 0.6$, $R = 2.5$ a.u. and $E_0 = 0.6$ a.u. at the field intensity $I = 1 \times 10^{14} \text{W/cm}^2$ (Figs. 2(a) and (c)) and $I = 1.5 \times 10^{14} \text{W/cm}^2$ (Figs. 2(b) and (d)). Figs. 2(a) and (b) are the numerical results and Figs. 2(c) and (d) are the analytic results calculated by Eq. (3). The harmonic spectra in Fig. 2 show a board and flat suppressed region, which is nearly spreading in the whole plateau region, as indicated by the horizontal arrows. In contrast, for the large internuclear distance cases as indicated by Fig. 1, the harmonic spectra show some kind of hump or dip structure. Especially as the field intensity increases, the hump structure become more pronounced around the 15th order harmonic in Figs. 1(b) with $I = 1 \times 10^{14} \text{W/cm}^2$, compared to that in Figs. 1(a) with $I = 5.3 \times 10^{13} \text{W/cm}^2$. Our calculations have been extended to the model molecules with $R = 10$ a.u. and

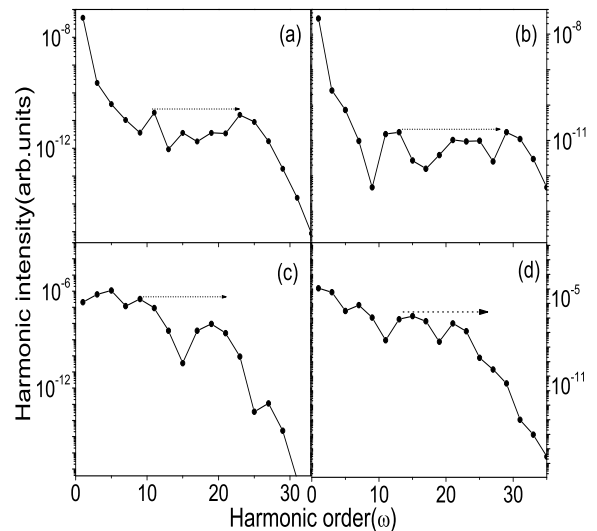


Figure 2: Photon-emission spectra of a symmetrical diatomic molecule with $Z = 0.6$, $R = 2.5$ a.u. and $E_0 = 0.6$ a.u. at the field intensity $I = 1 \times 10^{14} \text{W/cm}^2$ (Figs. 2(a) and (c)) and $I = 1.5 \times 10^{14} \text{W/cm}^2$ (Figs. 2(b) and (d)). (a) and (b): The numerical results; (c) and (d): the analytic results calculated by Eq. (3). See the context for the illumination of the arrows.

$R = 12$ a.u. at different laser intensity. They exhibit the similar phenomena as revealed in Fig. 1.

Fig. 3 shows the relationship of the momentum \mathbf{p} and the function

$$S_1(\mathbf{p}) = \langle 0 | \mathbf{p}_k \rangle (\mathbf{p} \cdot \hat{\mathbf{e}})^2 \langle \mathbf{p}_k | 0 \rangle, \quad (4)$$

for the chosen model molecule in Fig. 1. The arrows in it indicate those momenta at which the minimal extrema of Eq. (4) appear. The relevant momentum values are labelled above the arrows. The neighboring peaks and hollows in Fig. 3, corresponding to certain maximal and minimal extrema of Eq. (4), are very close.

According to the simple picture regarding the nuclei as point emitters proposed by Lein *et al*[2], for molecules with symmetric initial states, destructive interference (minimum in the harmonic spectrum) occurs when $p_k R \cos(\theta) = (2n + 1)\pi$, $n = 0, 1, 2, \dots$. Here $p_k = |\mathbf{p}_k|$ is the effective momentum of the electron, θ is the angle between the molecular axis and the laser polarization direction. Constructive interference (maximum in the harmonic spectrum) occurs when $p_k R \cos(\theta) = 2n\pi$, $n = 0, 1, 2, \dots$ [2, 4]. In the 1D case, for $R = 2.5$ a.u., the first predicted minimum is at the 13th order harmonic, which agrees with that in Figs. 2(a). While in Figs. 2(b), the minimum shifts to the 17th order harmonic. For the large $R = 16$ a.u., the predicted minima are at the 8th order with $n = 2$, the 16th order with $n = 3$, and the 27th order with $n = 4$, etc. The maxima are at the 12th order with $n = 3$ and the 21th order with

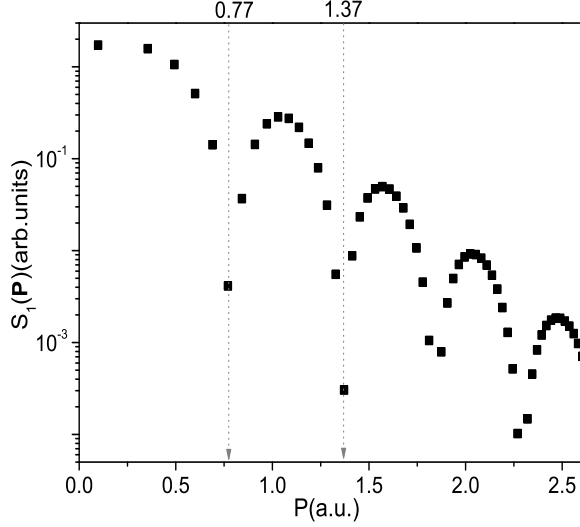


Figure 3: The relationship between the function $S_1(\mathbf{p})$ and the momentum \mathbf{p} for the chosen model molecule in Fig. 1. See the context for the illumination of the arrows and the numbers above the arrows.

$n = 4$, etc. While in the numerical cases, the pronounced minimum is at the 17th order in Figs. 1(a) and the 23th order in Figs. 1(b). The pronounced maximum is at the 15th order in Figs. 1(b). From the above observations, we find that the interference patterns in the HHG usually depend on the laser intensity. Moreover, for the large R case, it becomes difficult for the simple point-emitters model to predict the interference patterns.

To illuminate the hump and dip structure in Figs. 1(b), we investigate the physical mechanism for the emission of a harmonic order from molecules with large R . In Fig. 4, using the same laser and molecule parameters as in Figs. 1(b), we plot the values of $S_2(\mathbf{p})$ without considering the interference term Eq. (4) (the red curves with the hollow symbol) and $S(\mathbf{p})$ with considering the interference term Eq. (4) (the black curves with the solid symbol) as functions of the electron momentum \mathbf{p} for certain individual harmonic orders. Here

$$S_2(\mathbf{p}) = J_n\left(\frac{-\mathbf{p} \cdot \mathbf{A}_0}{\omega}\right) J_m\left(\frac{\mathbf{p} \cdot \mathbf{A}_0}{\omega}\right), \quad (5)$$

and

$$S(\mathbf{p}) = \langle 0|\mathbf{p}\rangle (\mathbf{p} \cdot \hat{\mathbf{e}})^2 \langle \mathbf{p}|0\rangle J_n\left(\frac{-\mathbf{p} \cdot \mathbf{A}_0}{\omega}\right) J_m\left(\frac{\mathbf{p} \cdot \mathbf{A}_0}{\omega}\right). \quad (6)$$

And only the contributions from positive momenta are shown. For clarity, we use the dotted arrows to indicate those momenta, which correspond to the first several minimal extrema of $S_1(\mathbf{p})$ in Fig. 3. The relevant momentum values are labelled above the arrows. We use the horizontal arrows in Figs. 4(a) to indicate several maximal extrema of $S_2(\mathbf{p})$ (denoted as $peak_1$ and $peak_2$).

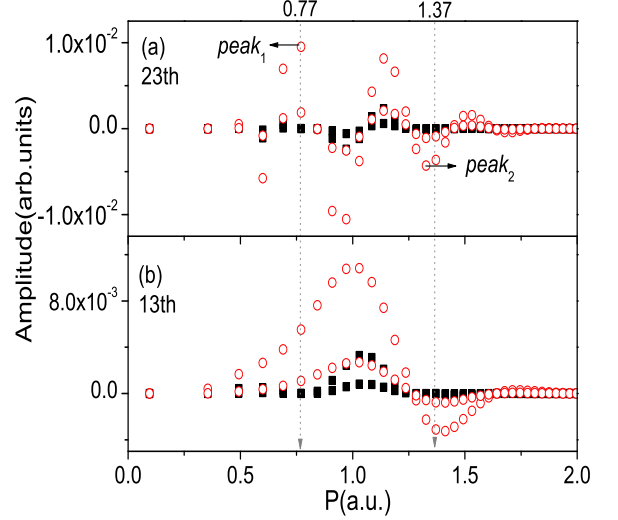


Figure 4: The values of $S_2(\mathbf{p})$ (the red curves with the hollow symbol) and $S(\mathbf{p})$ (the black curves with the solid symbol) as functions of the electron momentum \mathbf{p} for certain individual harmonic orders. Harmonic orders are as indicated. The laser and molecule parameters are the same as in Figs. 1(b). Only the contributions from positive momenta are shown. See the context for the illumination of the arrows and the numbers above the arrows.

From Eq. (6), the contributions to single peak of HHG consist of two parts, i.e., the interference term $S_1(\mathbf{p})$ and Bessel function term $S_2(\mathbf{p})$. For the 23th order harmonic at which the harmonic dip appears in Figs. 1(d), without considering the interference term $S_1(\mathbf{p})$, the primary contributions of $S_2(\mathbf{p})$ come from those momenta around the values of $p = 0.77$ a.u. and $p = 1.37$ a.u. corresponding to two of the minimal extrema of $S_1(\mathbf{p})$, as indicated by the red curve with the hollow symbol in Figs. 4(a). When considering the interference term $S_1(\mathbf{p})$, the contributions from those momenta are strongly suppressed, as indicated by the black curve with the solid symbol in Figs. 4(a). In Figs. 4(a) those momenta around the value of $p = 1.02$ a.u. give positive and negative contributions to the amplitude of the 23th order harmonic. Because the positive and negative values will cancel each other so the sum of these contributions is small.

For other harmonic orders, for example, the 13th order, around which the harmonic hump appears in Figs. 1(d). The red curve with the hollow symbol in Figs. 4(b) shows that the primary contributions of $S_2(\mathbf{p})$ to the harmonic order come from those momenta around the value of $p = 1.02$ a.u., different from $p = 0.77$ a.u. and $p = 1.37$ a.u. of the 23th order case. The black curve with the solid symbol in Figs. 4(b) also shows that the suppression effect from the interference term $S_1(\mathbf{p})$ is weaker than that of the 23th order case. The above

observations indicate that the interference term $S_1(\mathbf{p})$ is mainly responsible for the formation of the hump and dip in Figs. 1(b).

Fig. 4 clearly shows that the formation of single order harmonic is closely related to the recombination electrons with many different momenta \mathbf{p} . The contribution from the recombination electron at one certain momentum \mathbf{p} is weighted by the corresponding probability amplitude $S(\mathbf{p}) = S_1(\mathbf{p})S_2(\mathbf{p})$. In addition, from Figs. 4(a) it can also be concluded that the interference minimum in the harmonic spectrum could appear at the harmonic order at which the primary contributions from the term $S_2(\mathbf{p})$ are strongly suppressed due to the destructive interference from the term $S_1(\mathbf{p})$. Since the probability amplitude $S(\mathbf{p})$ depends on the field intensity, the position of the harmonic hump or dip depends on the intensity too.

The interference patterns in HHG for molecules with large R are much more complicated than that for molecules with small R . The adjacent maximal and minimal extremum points of $S_1(\mathbf{p})$ correspond to constructive and destructive interferences. They are so close as shown in Fig. 3, that the constructive and destructive interference extrema in the plottings of $S(\mathbf{p})$ could be entangled. This makes the interference effects on HHG very sensitive to the field intensity. In this case, the simple point-emitter model is not available. Our model could provide

a good description for the HHG of diatomic molecules even for the case of large internuclear separation.

IV. CONCLUSION

In conclusion, using a SFA model that considers Coulomb potential modification on the continuum wavefunctions, we have analytically and numerically investigated the HHG from diatomic molecules with large internuclear separation. The harmonic spectra obtained by the SFA model agree with the numerical simulations. Our model calculation reveals that the two-center interference as well as the interference between different recombination electron trajectories are responsible for the unusual enhanced or suppressed harmonic yield at a certain order, and these interference effects depend on the laser parameters such as intensity

V. ACKNOWLEDGEMENTS

This work is supported by 973 research program No. 2006CB806000, NNSF(No.10725521).

-
- [*] Liu_Jie@iapcm.ac.cn
- [1] M. Lein, N. Hay, R. Velotta, J. P. Marangos, and P. L. Knight, Phys. Rev. Lett **88**, 183903, (2002).
- [2] M. Lein, N. Hay, R. Velotta, J. P. Marangos, and P. L. Knight, Phys. Rev. A. **66**, 023805 (2002).
- [3] M. Lein, P. P. Corso, J. P. Marangos, and P. L. Knight, Phys. Rev. A. **67**, 023819 (2003).
- [4] G. Lagmago Kamta and A. D. Bandrauk, Phys. Rev. A **71**, 053407 (2005).
- [5] Anh-Thu Le, X.-M. Tong, and C. D. Lin, Phys. Rev. A **73**, 041402(R) (2006).
- [6] R. de Nalda, E. Heesel, M. Lein, N. Hay, R. Velotta, E. Springate, M. Castillejo, and J. P. Marangos, Phys. Rev. A **69**, 031804(R) (2004).
- [7] C. Vozzi, F. Calegari, E. Benedetti, J.-P. Caumes, G. Sansone, S. Stagira, M. Nisoli, R. Torres, E. Heesel, N. Kajumba, J. P. Marangos, C. Altucci and R. Velotta, Phys. Rev. Lett. **95**, 153902 (2005).
- [8] Kanai, Tsuneto, Minemoto, Shinichirou, and Sakai. Hirofumi, Nature **435**, 470-473(2005).
- [9] P. Dietrich, M. Yu. Ivanov, F. A. Ilkov, and P. B. Corkum, Phys. Rev. Lett. **77**, 4150(1996)
- [10] X. X. Zhou, X. M. Tong, Z. X. Zhao, and C. D. Lin, Phys. Rev. A. **72**, 033412 (2005).
- [11] J. Itatani, D. Zeidler, J. Levesque, Michael Spanner, D. M. Villeneuve, and P. B. Corkum, Phys. Rev. Lett **94**, 123902(2005).
- [12] Yanjun Chen, Jing Chen, and Jie Liu, Phys. Rev. A. **74**, 063405 (2006).
- [13] M. F. Ciappina, C. C. Chirila. and M. Lein, Phys. Rev. A **75**, 043405 (2007)
- [14] J. Chen and S. G. Chen, Phys. Rev. A. **75**, 041402(R) (2007).
- [15] J. Itatani, J. Levesque, D. Zeidler, Hiromichi Niikura, J. C. Kieffer, P. B. Corkum, and D. M. Villeneuve, Nature **432**, 867(2004).
- [16] M. Hentschel *et al.*, Nature(London) **414**, 509(2001); M. Drescher *et al.*, *ibid.* **419**, 803(2002); Z. Chang *et al.*, Phys. Rev. Lett. **79**, 2967(1997).
- [17] P. B. Corkum, Phys. Rev. Lett. **71**, 1994 (1993).
- [18] M. Lewenstein, Ph. Balcou, M. Yu. Ivanov, Anne L'Huillier and P. B. Corkum, Phys. Rev. A **49**, 2117(1994).
- [19] J. Levesque, D. Zeidler, J. P. Marangos, P. B. Corkum, and D. M. Villeneuve, Phys. Rev. Lett. **98**, 183903 (2007).
- [20] V. I. Usachenko, V. A. Pazdersky, and J. K. Mciver, Phys. Rev. A **69**, 013406 (2004)
- [21] J. Muth-Bohm, A. Becker, and F. H. M. Faisal, Phys. Rev. Lett. **85**, 2280(4) (2000)
- [22] Bambi Hu, Baowen Li, Jie Liu, and Yan Gu, Phys. Rev. Lett. **82**, 4224 (1999); Bambi Hu, Baowen Li, Jie Liu, and Ji-Lin Zhou, Phys. Rev. E **58**, 1743 (1998).